Since January 2020 Elsevier has created a COVID-19 resource centre with free information in English and Mandarin on the novel coronavirus COVID-19. The COVID-19 resource centre is hosted on Elsevier Connect, the company's public news and information website.

Journal of Pharmaceutical and Biomedical Analysis 187 (2020) 113356

Contents lists available at ScienceDirect

Journal of Pharmaceutical and Biomedical Analysis

journal homepage: www.elsevier.com/locate/jpba

Stereoselective pharmacokinetic study of epiprogoitrin and progoitrin in rats with UHPLC–MS/MS method

Yan Xu[a], Jinhang Li[a], Yanhong Shi[b], Li Yang[c,d], Zhengtao Wang[d], Han Han[a,e,*], Rui Wang[a,*]

[a] School of Pharmacy, Shanghai University of Traditional Chinese Medicine, Shanghai 201203, China
[b] Institute of TCM International Standardization, Shanghai University of Traditional Chinese Medicine, Shanghai 201203, China
[c] Institute of Interdisciplinary Integrative Medicine Research, Shanghai University of Traditional Chinese Medicine, Shanghai 201203, China
[d] The MOE Key Laboratory of Standardization of Chinese Medicines, Institute of Chinese Materia Medica, Shanghai University of Traditional Chinese Medicine, Shanghai 201203, China
[e] Experiment Center for Teaching and Learning, Shanghai University of Traditional Chinese Medicine, Shanghai 201203, China

ARTICLE INFO

Article history:
Received 26 December 2019
Received in revised form 16 April 2020
Accepted 3 May 2020
Available online 7 May 2020

Keywords:
Epiprogoitrin
Progoitrin
Pharmacokinetics
Stereospecific
LC–MS/MS

ABSTRACT

An accurate and precise liquid chromatography–electrospray ionization–tandem mass spectrometry (LC–ESI–MS/MS) method was developed and validated for the pharmacokinetic study of epiprogoitrin and progoitrin, a pair of epimers that can be deglycosylated to epigoitrin and goitrin, respectively. These analytes were administered intravenously or intragastrically to male Sprague–Dawley rats, and the influence of 3(R/S)-configuration on the pharmacokinetics of both epimers in rat plasma was elucidated. The analytes and an internal standard (i.e., sinigrin) were resolved by LC–MS/MS on a reverse-phase ACQUITY UPLC™ HSS T3 column equilibrated and eluted with acetonitrile and water (0.1 % formic acid) at a flow rate of 0.3 mL/min. Quantitation was achieved by applying the multiple reaction monitoring mode, in the negative ion mode, at transitions of *m/z* 388 → 97 and *m/z* 358 → 97 for the epimers and sinigrin, respectively. The method demonstrated good linearity over the concentration range of 2–5000 ng/mL ($r > 0.996$). The lower limit of quantification for epiprogoitrin and progoitrin was 2 ng/mL. The interday and intraday accuracy and precision were within ±15 %. The extraction recovery, stability, and matrix effect were demonstrated to be within acceptable limits. The validated method was thus successfully applied for the pharmacokinetic study of both the epimers. After the rats received the same oral dose of the epimers, the pharmacokinetic profiles were similar. The maximum plasma concentration (C_{max}) and AUC values of epiprogoitrin were a bit higher than those of progoitrin, whereas the pharmacokinetic behaviours of the epimers were obviously different upon intravenous administration. The C_{max} and AUC values of epiprogoitrin were approximately three-fold higher than those of progoitrin, and the half-life of progoitrin was much shorter than that of epiprogoitrin. The oral bioavailability of progoitrin was 20.1 %–34.1 %, which is three times higher than that of epiprogoitrin.

1. Introduction

Radix isatidis is the dry root of *Isatis indigotica* Fort. (Brassicaceae) and is one of the traditional Chinese herbs that is extensively used for the treatment of colds, fever, and influenza. In recent years, granules, eye drops, syrups, and even functional beverages developed from *R. isatidis* have been introduced into the market [1,2]. Notably, it has also been employed for the treatment of severe acute respiratory syndrome (SARS) and H_1N_1-influenza [3,4].

Relevant studies have shown that progoitrin, epiprogoitrin, and their derivatives (goitrin and epigoitrin) are the main glucosinolates in *R. isatidis*; these chemical constituents reportedly exhibit many biological activities, including antiviral, anti-inflammatory, and anticancer effects [5–7]. In addition, progoitrin, epiprogoitrin, goitrin, and epigoitrin account for 34 %, 60 %, 3%, and 1.8 % of total glucosinolates, respectively [8]. Epiprogoitrin and progoitrin are converted to corresponding aglycones and other degradation products (epigoitrin/goitrin) by enzymatic hydrolysis through myrosinase in plants or enzymes in the gastrointestinal tract, and this the main biosynthetic pathway of goitrin and epigoitrin [9]. Moreover, epiprogoitrin and progoitrin bear a chiral carbon at C-3 as part of their structural skeleton, forming a pair of optical epimers, namely progoitrin (R-progoitrin) and epiprogoitrin (S-progoitrin),

* Corresponding authors at: Experiment Center for Teaching and Learning, Shanghai University of Traditional Chinese Medicine, Shanghai 201210, China.
E-mail addresses: pashanhan@126.com (H. Han), ellewang@163.com (R. Wang).

https://doi.org/10.1016/j.jpba.2020.113356
0731-7085/

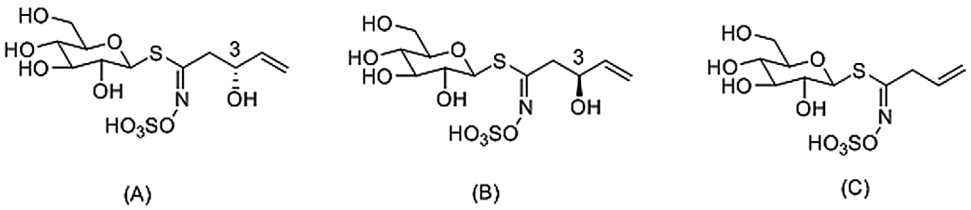

Fig. 1. Chemical structures of (A) progoitrin (R-progoitrin), (B) epiprogoitrn (S-progoitrin) and (C) sinigrin (internal standard).

respectively (Fig. 1A, B). Although the mechanisms underlying these stereoselective functions remain unclear, numerous studies have demonstrated that such epimers [20(S)-ginsenoside Rg_3 and 20(R)-ginsenoside Rg_3 in *Panax notoginseng*] exhibit various stereoselective activities, such as effects on the cardiovascular [10] and immune system [11], and antitumor [12,13] and antidiabetic activities [14]. These findings suggest that the stereostructure of the alkane chains is responsible for different pharmacokinetic characteristics and even diverse metabolism patterns after administration.

In previous study, a reversed-phase HPLC method was developed that led to the identification of 12 intact glucosinolates, including progoitrin and epiprogoitrin, in traditional Chinese plants [6]. In addition, Shi et al. reported an optimized efficient method of HPLC-UV-CD to simultaneously separate and quantify the four main chiral glucosinolates: progoitrin, epiprogoitrin, and R,S-goitrin in crude drugs, decoction pieces, and granules of *R. Isatidis* [15]. Recently, a fast, selective, and sensitive LC–MS/MS method coupled with acetonitrile-mediated protein precipitation was recently introduced for detecting (R, S)-goitrin in rat plasma [16]. However, to date, no method for the quantification of progoitrin or epiprogoitrin in biological samples has been reported; information on the pharmacokinetics of glucosinolates in *R. isatidis*, particularly progoitrin and epiprogoitrin, is insufficient; consequently, no study has yet performed a systematic comparison of the pharmacokinetics of progoitrin and epiprogoitrin. These obstacles have thus hindered their application.

Accordingly, establishing a simple, reliable method for the pharmacokinetic study of progoitrin and epiprogoitrin is pivotal. This study aimed to develop a method for the pharmacokinetic study of epiprogoitrin and progoitrin both after intravenous (i.v.) and intragastric (i.g.) administrations and to elucidate the influence of 3 (R/S)-configuration on the pharmacokinetics of epiprogoitrin and progoitrin.

2. Material and Methods

2.1. Chemical and reagents

Progoitrin and epiprogoitrin ($C_{11}H_{19}NO_{10}S_2$, Fig. 1A, B) with purity levels of >98 % was obtained from Shanghai U-Sea Biotech Co., Ltd. (Shanghai, China), and sinigrin (internal standard, $C_{10}H_{17}NO_9S_2$, Fig. 1C) with purity levels of >98 % was purchased from Sigma-Aldrich Co., LLC (St. Louis, MO, USA). HPLC-grade acetonitrile and methanol were obtained from Merck (Darmstadt, Germany). Water used in each step was freshly prepared with a Millipore water purification system (MA, USA). All other chemicals and reagents were of analytical grade and commercially available.

2.2. Animals and sampling

Male Sprague–Dawley rats (7–8 weeks old, 200–250 g) were purchased from the Laboratory Animal Center of Shanghai University of Traditional Chinese Medicine (Shanghai, China) and kept in a light- and temperature-controlled room (room temperature, 21 °C – 22 °C; relative humidity, 60 %–65 %; 12/12 h light/dark cycle) for 7 days before experiment initiation to adapt them to the laboratory housing conditions. The animals were fed a standard diet and provided ad libitum access to food and tap water. All experimental procedures were approved by the Ethics Committee of Shanghai University of Traditional Chinese Medicine. Animal welfare and experimental procedures were strictly in accordance with the guidelines of the Animal Ethics Committee of Shanghai University of Traditional Chinese Medicine (process number: PZSHUTCM19032501).

A total of 48 male Sprague–Dawley rats were randomly assigned to two groups (namely epiprogoitrin and progoitrin), and the 24 rats in each group were randomised into four groups (n = 6) depending on the i.v. and i.g. administration of epiprogoitrin or progoitrin in different dosages. For i.v. administration, 5 mg of epiprogoitrin (progoitrin) was dissolved in 5 mL water, and each of the six rats received 2 mg/kg through the caudal vein within 1 min. The other three groups of rats were subjected to i.g. administration of 20, 25, or 30 mg/kg epiprogoitrin (progoitrin) dissolved in water. All dosing solutions were prepared immediately before administration. Blood samples (200 μL) were obtained from the periorbital sinus vein before administration (0 h) and 0.083, 0.25, 0.5, 0.75, 1, 1.5, 2, 4, 6, 8, and 12 h after administration. The blood samples were then centrifuged at 6000 rpm for 10 min at 4 °C. The reulting plasma thus obtained was transferred into a clean 1.5 mL polypropylene tube and stored at −80 °C until needed.

2.3. LC–MS/MS system and conditions

Epiprogoitrin and progoitrin were quantitated using a Shimadzu LCMS-8050 triple quadrupole mass spectrometer coupled with an electrospray ionization (ESI) interface (Shimadzu, Tokyo, Japan). The mass spectrometer was operated in the negative ion mode, and the operating parameters were optimised as follows: nebuliser gas flow, 3 L/min; heating gas flow, 10 L/min; drying gas flow, 10 L/min; interface temperature, 300°C; desolvation line temperature, 250°C; and heat block temperature, 400°C. The ESI–MS/MS parameters are listed in Table 1. The descriptions of qualifier transitions for the method including the MS/MS spectra of epiprogoitrin and progoitrin as well as IS are described in Fig. 2. Quantitation was achieved according to the multiple reaction monitoring (MRM) mode. Analytical data were processed with LabSolutions v2.0 (Shimadzu).

The processed samples (5 μL) were injected into an ACQUITY UPLC™ HSS T3 column (100 × 2.1 mm i.d., 1.8 μm; Waters Corporation, Milford, MA, USA) maintained at 45 °C. The autosampler tray was maintained at 10 °C, and the sample injection volume was 5 μL. Acetonitrile (A) and 0.1 % aqueous formic acid (B) were used as the gradient mobile phase with a flow rate of 0.3 mL/min. The gradient elution programme was set as follows: 0–2 min, 95 % B; 2–3 min, 5% B; 3–4 min, 95 % B; and finally 95 % B for 0.3 min for reconditioning the column. The total chromatographic time was 4 min, and the retention times of epiprogoitrin, progoitrin, and IS were 1.51, 1.30, and 1.72 min, respectively.

Table 1
MRM parameters of epiprogoitrin, progoitrn and IS (negative ion mode).

Analytes	Precursor ion (m/z)	Product ion (m/z)	Collision energy (V)	Q1 Pre Bias (V)	Q3 Pre Bias (V)
Epiprogoitrin/progoitrin	388	97	21	19	17
Sinigrin(IS)	358	97	21	17	10

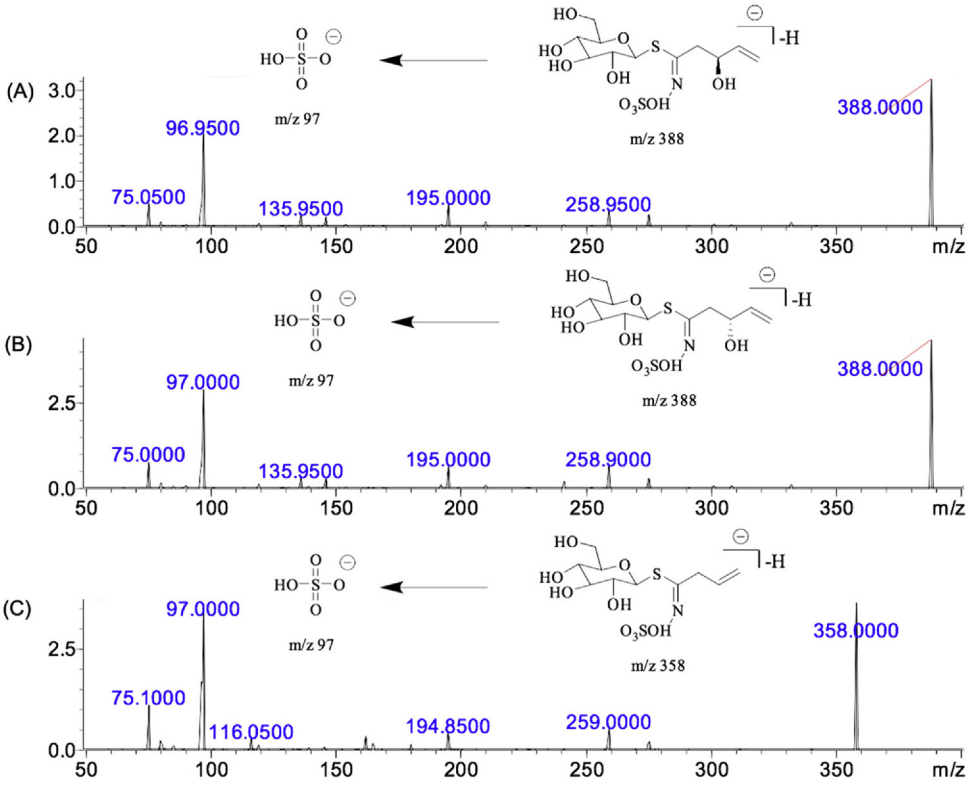

Fig. 2. MS/MS spectrum of epiprogoitrin (A), progoitrin (B) and IS (C).

2.4. Stock and working solutions

Standard stock solutions of sinigrin (IS), epiprogoitrin, and progoitrin (5 mg/mL) were prepared using pure water. The standard solutions with different concentrations were then serially diluted with pure water and protected from light. All solutions were stored at 4 °C until further analyses.

2.5. Sample pretreatment

An aliquot of 50 μL IS working solution (200 ng/mL) was dried under N_2 and spiked with 50 μL plasma in a 1.5 mL Eppendorf tube. To this mixture, 250 μL acetonitrile was added. After this solution was vortexed for 30 s, it was centrifuged at 13,500 rpm for 10 min at 4 °C. Subsequently, 150 μL of the clear upper layer was transferred to another 1.5 mL Eppendorf tube for each extract and then dried under N_2; the dried residues were reconstituted in 200 μL pure water and centrifuged at 13,500 rpm for 10 min at 4 °C. The supernatant was then transferred to vials for LC–MS/MS analyses.

2.6. Method validation

Method validation was conducted on the basis of the currently accepted FDA prescription and per guidelines of the International Conference on Harmonization of Technical Requirements for Registration of Pharmaceuticals for Human Use [17].

2.6.1. Selectivity

The selectivity of the method was assessed by comparing MRM chromatograms of six different batches of blank plasma samples from six rats, blank plasma samples from rats spiked with the analytes at LLOQ, and a plasma sample obtained 1 h after oral administration of 25 mg/kg epiprogoitrin/progoitrin. No endogenous substances interfered with the retention times of either analytes or IS.

2.6.2. Calibration and lower limit of quantification

The lower limit of quantification (LLOQ) was defined as the lowest concentration of the calibration curve with acceptable precision (<15 %) and accuracy (within ±20 %) at which the signal-to-noise ratio was determined to be >10. The calibration curves were constructed using 12 calibration standards over the range of 2–5000 ng/mL by plotting the peak area ratio of analytes to IS (200 ng/mL) (y) versus the nominal concentrations of analytes (x) in plasma using a $1/x^2$ weighted linear least-square regression model. The calibration curve was expected to have a correlation coefficient (r) of >0.99.

2.6.3. Precision and accuracy

Accuracy and precision were evaluated using quality control (QC) samples at three concentrations (5, 100, and 4000 ng/mL; n = 6) and LLOQ concentration (2 ng/mL; n = 6) on the same day and over three consecutive days. The calibration curves and samples were prepared and analysed on the same day. The accuracy of the method was calculated as the relative error (RE) and was required to be

within ±15 %, whereas the precision of the method was expressed in terms of relative standard deviation (RSD) and was required to be <15 %.

2.6.4. Stability

The stability of epiprogoitrin and progoitrin in rat plasma was assessed by analysing replicates (n = 6) at three QC concentrations (5, 100, 4000 ng/mL) and LLOQ concentration (2 ng/mL) under various storage conditions and processing procedures. Short-term stability was determined after sample storage at room temperature for 24 h, and long-term stability was assessed by evaluating the QC samples stored at −20 °C for 2 weeks. To assess freeze–thaw stability, the samples were subjected to three freeze – thaw cycles between −80 °C and room temperature. Autosampler stability was assessed by analysing samples left in the autosampler at 10 °C for 8 h. The calibration curves of freshly prepared standards were used for all stability tests of QC samples.

2.6.5. Extraction recovery and matrix effects

The extraction recovery of the analytes and IS from rat plasma were assessed at three QC concentrations (5, 100, and 4000 ng/mL; n = 6) and LLOQ concentration (2 ng/mL; n = 6), were calculated by comparing the area response in extracted samples with post extraction blanks spiked with equivalent concentration of analyte solution. The matrix effects at three QC concentrations (5, 100, and 4000 ng/mL; n = 6) and LLOQ concentration (2 ng/mL; n = 6) were measured by comparing peak responses of samples spiked after extraction (A) with those of pure water containing equivalent amounts of each analyte and IS (B). The ratio (A/B × 100 %) was used to evaluate the matrix effects. The extraction recoveries and matrix effects of IS were simultaneously evaluated at 200 ng/mL by using the same method.

2.7. Pharmacokinetic analysis

The following pharmacokinetic parameters were calculated using a noncompartmental pharmacokinetic model in DAS 3.1 (BioGuider Co., Shanghai, China): the maximum plasma concentrations (C_{max}), the time to reach C_{max} (T_{max}), total body clearance (CL), volume of distribution (Vd), mean residence time (MRT) were obtained directly from the experimental data. The elimination rate constant (k_e) was calculated using log-linear regression of the terminal portion of each curve. The elimination half-life ($t_{1/2}$) was calculated as $0.693/k_e$. The area under the curve [$AUC_{0\text{-}t}$, from 0 to the last measurable plasma concentration (C_t)] was calculated using the linear trapezoidal method and was extrapolated to infinity [$AUC_{(0-\infty)}$] using the following formula: $AUC_{0\text{-}\infty}=AUC_{0\text{-}t}+C_t/k_e$. Oral bioavailability was defined as the fraction of unchanged drug reaching the systemic circulation following administration through the i.g. route and was measured using the following equation: $F(\%) = (AUC_{i.g.} \times Dose_{i.v.})/(AUC_{i.v.} \times Dose_{i.g.}) \times 100\ \%$.

3. Results and Discussion

3.1. Assay development and performance

To develop an accurate, sensitive method for analysing epiprogoitrin/progoitrin, sample preparation is critical for developing a time-saving and effective LC–MS/MS assay. When recovering drugs from matrices, it is vital to use a valid extraction procedure to exclude or minimise matrix interferences. Sample preparation methods, including protein precipitation, solid phase extraction, and liquid–liquid extraction, have been investigated. After evaluating, acetonitrile-mediated precipitation is a better opt, which produced low consumption and achieved good sensitivity in analysis.

Triple quadrupole in MRM mode has become a widely used method. A standard solution was injected into the mass spectrometer to ascertain precursor ions and select product ions using LabSolutions software. A full scan of epiprogoitrin/progoitrin and IS produced molecular ions $[M-H]^-$ at *m/z* 388 and 358, respectively, and detection in the negative ion mode was more stable than that in the positive ion mode.

In addition, the composition of the mobile phase can influence peak shape and ionization efficiency. Using a gradient mobile phase of acetonitrile and water has been proven to be effective, and the addition of formic acid in water and acetonitrile were used to separate and elute analytes, which combined to produce symmetric chromatographic peaks and provide good separation, when compared with 5 mmol ammonium acetate and other mobile phase. Thus, it is a suitable method for analyses due to the short anlysis time, economic sample pretreatment steps and high sensitivity.

3.2. Method validation

3.2.1. Specificity

Specificity was evaluated by comparing MRM chromatograms of blank plasma samples to corresponding spiked plasma samples. The representative chromatograms of blank plasma, spiked plasma samples (LLOQ), and plasma samples after oral administration of the analytes are shown in Fig. 3. It is obvious that no endogenous substances interfered with the ionization of the analytes in any sample. The retention times for epiprogoitrin, progoitrin, and IS were 1.51, 1.40, and 1.72 min, respectively.

3.2.2. Calibration curve and LLOQ

The calibration curves were established by plotting the ratios of chromatogram peak areas of the analytes to IS. Good linearity was achieved over the concentration range of 2–5000 ng/mL ($r > 0.996$). The regression equations for epiprogoitrin and progoitrin were $y = 0.0066x + 0.0041$ ($r > 0.999$) and $y = 0.0061x + 0.0010$ ($r > 0.996$), respectively, where y represents the peak area ratio of the analytes to IS and x denotes the concentration of analytes in the plasma.

The LLOQ for epiprogoitrin/progoitrin was 2 ng/mL based on a signal-to-noise ratio of >10. The lower limit of detection (LOD) was estimated to be 1 ng/mL (S/N > 3), and the accuracy (RE) and precision (RSD) at LLOQ were 12.7 % and 10.5 %, respectively.

3.2.3. Precision and accuracy

The intra-day and inter-day accuracy (RE) and precision (RSD) of the analytes in rat plasma at three QC concentrations (5, 100, 4000 ng/mL) and LLOQ concentration (2 ng/mL; n = 6) are shown in Tables S1 and S2 which followed the guidelines of biologic samples set by the FDA, it suggests that accuracy and precision should be within ±15 %.

3.2.4. Stability

The stability of the analytes was assessed under different experimental conditions (Table S3). At each QC concentration, the REs of the short-term, long-term, freeze–thaw, and autosampler stabilities were < 12.88 %. The obtained results from all stability tests demonstrated that the analytes were stable under diverse conditions; hence, the method was judged to be suitable for routine analysis.

3.2.5. Extraction recovery and matrix effects

The extraction recovery and matrix effects were evaluated to determine the reproducibility of the method. The mean extraction recoveries of epiprogoitrin and progoitrin at the three QC concentrations were > 91.30 % (Table S4). With respect to the matrix effect, the values ranged from 91.18 % to 107.27 % for all samples.

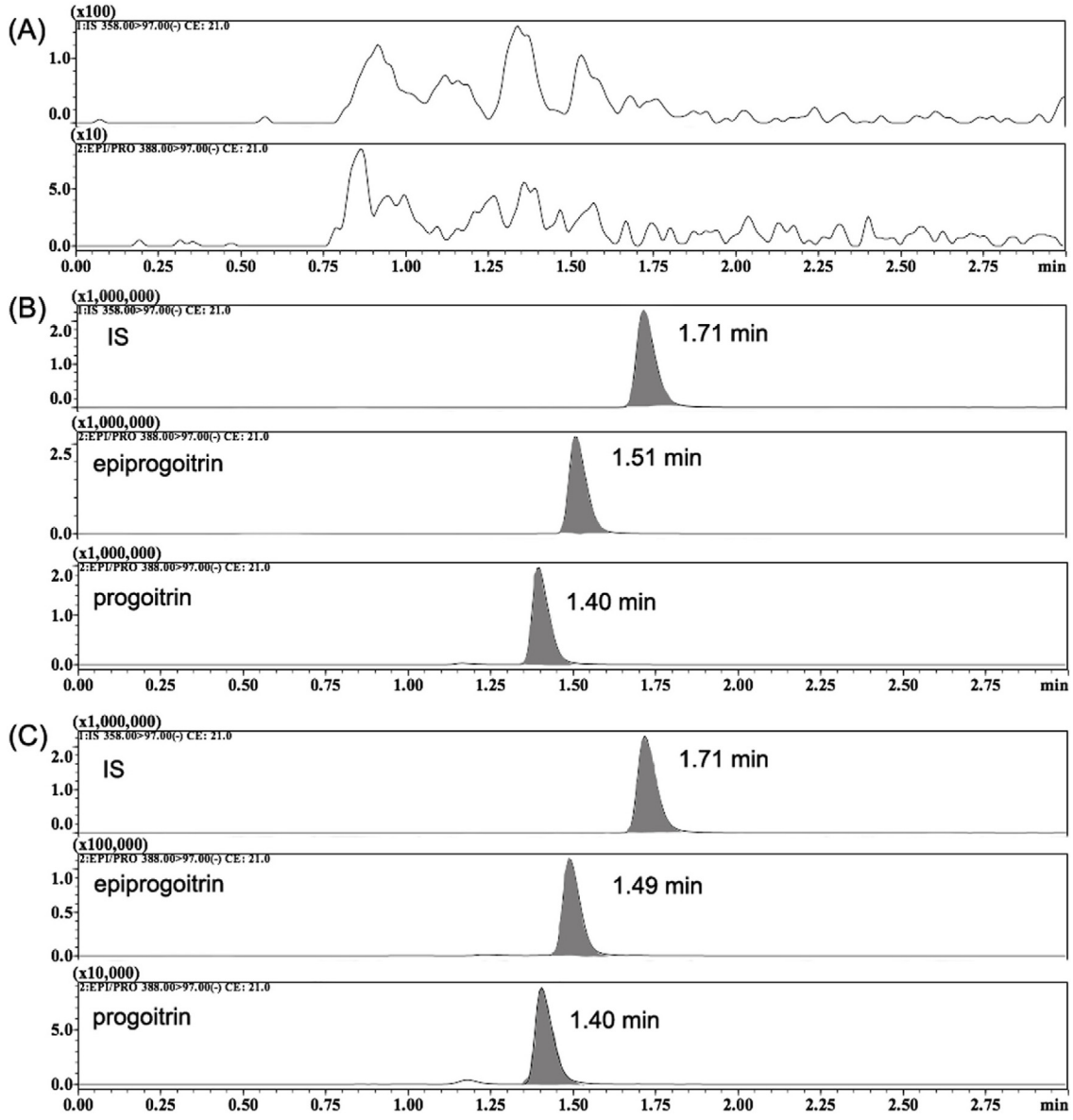

Fig. 3. The typical MRM chromatograms of epiprogoitrin, progoitrin and IS in rat plasma sample: (A) blank plasma sample, (B) blank plasma samples spiked with IS (200 ng/mL), epiprogoitrin and progoitrin respectively (2 ng/mL), (C) plasma samples at 1 h after a single oral administration of analytes (25 mg/kg).

The validation results indicated that the pretreatment process was efficient and reproducible; in addition, no endogenous substances from plasma significantly affected the analysis.

3.3. Application to pharmacokinetic study

3.3.1. Pharmacokinetics of epiprogoitrin and progoitrin after i.g. administration

The validated method was successfully applied to pharmacokinetically analyse epiprogoitrin and progoitrin after their oral administration (20, 25, or 30 mg/kg) to rats.

At the same dosage, similar plasma concentration–time curves for both epimers were obtained. The mean plasma concentration–time profiles are depicted in Fig. 4, and relevant pharmacokinetic parameters are summarised in Table 2.

Observation and comparison of relevant pharmacokinetic parameters at the same dosage yielded interesting results. As shown in Fig. 4 and Tables 2 and 3, epiprogoitrin and progoitrin were rapidly absorbed from the gastrointestinal tract after administration and were detectable in plasma from the first blood sampling time point (5 min); subsequently, the plasma concentration sharply increased to reach its peak in approximately 90 min. Epiprogoitrin and progoitrin were rapidly eliminated from the body over a period of approximately 2 h. The AUC and C_{max} val-

Table 2
Pharmacokinetic parameters of epiprogoitrin after oral administration (n = 6) at the doses of 20, 25, and 30 mg/kg. Data were expressed as mean ± S.D.

	20 mg/kg	25 mg/kg	30 mg/kg
C_{max}(μg/L)	700.21 ± 177.50	745.42 ± 303.17	1001.95 ± 179.38
T_{max}(h)	1.5 ± 0.55	1.39 ± 0.56	1.42 ± 0.65
AUC_{0-t}(μg/L*h)	2327.36 ± 477.85	2843.43 ± 448.06	3299.57 ± 617.90
$AUC_{0-\infty}$(μg/L*h)	2330.82 ± 478.32	2840.92 ± 447.86	3301.09 ± 617.47
$t_{1/2}$(h)	1.13 ± 0.30	1.33 ± 0.33	0.97 ± 0.14
MRT_{0-t}(h)	2.27 ± 0.070	2.28 ± 0.25	2.52 ± 0.07
$MRT_{0-\infty}$(h)	2.28 ± 0.067	2.30 ± 0.25	2.52 ± 0.07
Vd(L/kg)	15.33 ± 4.64	14.57 ± 6.69	13.42 ± 4.40
CL(L/kg/h)	9.55 ± 2.42	9.23 ± 2.19	9.41 ± 2.07
F(%)	9.3	7.3	8.7

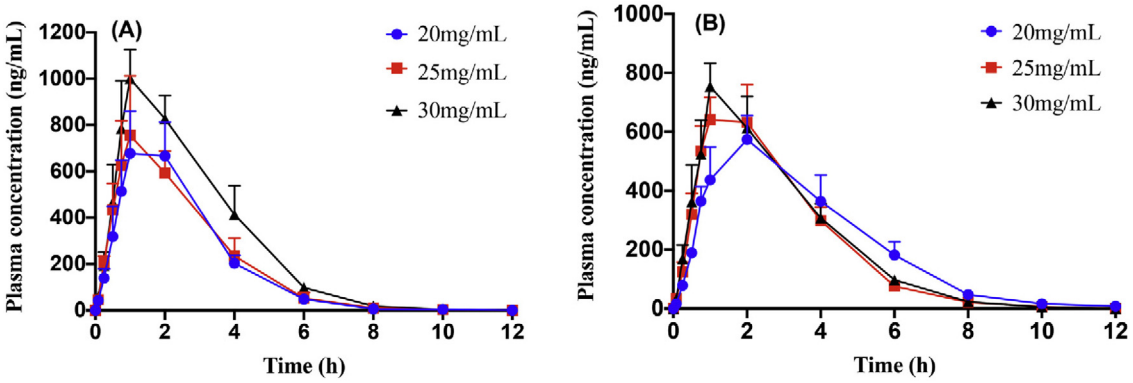

Fig. 4. Mean plasma concentration-time curves of epiprogoitrin (A, n = 6) and progoitrin (B, n = 6) after oral administration at the doses of 20, 25, and 30 mg/kg. Vertical bars represent standard deviation.

Table 3
Pharmacokinetic parameters of progoitrin after oral administration (n = 6) at the doses of 20, 25, and 30 mg/kg. Data were expressed as mean ± S.D.

	20 mg/kg	25 mg/kg	30 mg/kg
C_{max}(μg/L)	597.29 ± 161.09	677.98 ± 44.03	740.30 ± 103.27
T_{max}(h)	2.10 ± 0.51	1.33 ± 0.52	1.29 ± 0.56
$AUC_{0\text{-}t}$(μg/L*h)	2190.49 ± 399.70	2295.82 ± 364.48	2427.18 ± 331.66
$AUC_{0\text{-}\infty}$(μg/L*h)	2191.51 ± 403.48	2297.97 ± 364.54	2430.31 ± 331.97
$t_{1/2}$(h)	1.17 ± 0.15	0.99 ± 0.1	1.12 ± 0.08
$MRT_{0\text{-}t}$(h)	2.59 ± 0.23	2.61 ± 0.07	2.63 ± 0.08
$MRT_{0\text{-}\infty}$(h)	2.60 ± 0.22	2.62 ± 0.07	2.65 ± 0.08
Vd(L/kg)	12.85 ± 1.79	13.89 ± 2.7	21.06 ± 2.97
CL(L/kg/h)	7.69 ± 1.21	8.74 ± 1.35	8.09 ± 1.86
F(%)	34.1	26.9	20.1

ues of epiprogoitrin were always higher than those of progoitrin at the same dosage. The peak concentration was higher when a high dose of epiprogoitrin and progoitrin was administered (1001.95 ± 179.38 vs. 740.30 ± 103.27 μg/L) than when a medium (745.42 ± 303.17 vs. 677.98 ± 44.03 μg/L) or low (700.21 ± 177.50 vs. 597.29 ± 161.09 μg/L) dose was administered.

Tables 2 and 3 reveal that a single dose of orally administrated epiprogoitrin or progoitrin exhibited dose-dependent pharmacokinetic profiles in rats ($r^2 > 0.98$). None of the other pharmacokinetic parameters, such as $t_{1/2}$, T_{max}, MRT, CL, and Vd exhibited significant differences among the three concentrations ($p > 0.05$).

3.3.2. *Pharmacokinetics of epiprogoitrin and progoitrin after i.v. administration*

After rats were given an i.v. injection of epiprogoitrin and progoitrin, both evidently travel in the systemic circulation mainly as themselves; however, this may not be the case upon their i.v. administration. Epiprogoitrin and progoitrin demonstrated significant differences in pharmacokinetic parameters after administration.

Fig. 5 and Table 4 indicate that the pharmacokinetic profile of epiprogoitrin was obviously different from that of progoitrin; the C_{max} and AUC values of epiprogoitrin were approximately three-fold higher than those of progoitrin. The half-life of progoitrin was much shorter than that of epiprogoitrin, indicating that progoitrin is more easily eliminated from plasma than epiprogoitrin following a single i.v. administration. Moreover, the CL values of epiprogoitrin were approximately one-third of those of progoitrin. The oral bioavailability of epiprogoitrin and progoitrin also exhibited significant differences. The calculated absolute bioavailability of progoitrin was approximately three-fold higher than that of epiprogoitrin.

In terms of epiprogoitrin, the highest dosage was 30 mg/kg in oral administration, which was nearly ten-fold higher than the

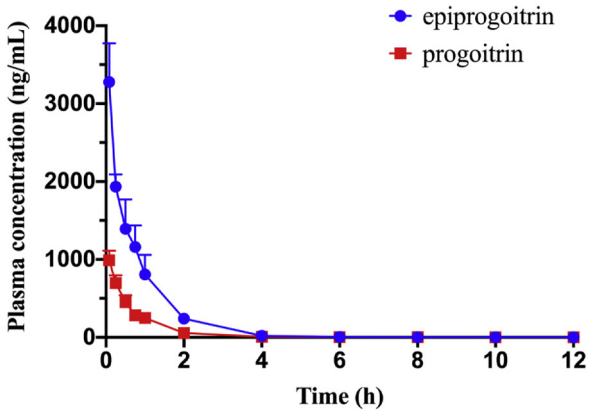

Fig. 5. Mean plasma concentration-time curves of epiprogoitrin and progoitrin after intravenous administration at the dose of 2 mg/kg (n = 6). Vertical bars represent standard deviation.

dosage of i.v. administration, the value of C_{max} after i.v. administration (3276.483 ± 497.368 μg/L) was truly larger than that after oral administration (1001.95 ± 179.38 μg/L) and the value of CL after oral administration (9.41 ± 2.07 L/kg/h) was faster than after i.v. administration (0.79 ± 0.092 L/kg/h). Therefore, after oral administration, epiprogoitrin was cleared faster than after i.v. administration in the body, and the value of $t_{1/2}$ after i.v. administration was higher than that after oral administration.

From the aforementioned results, it is evident that there exist differences between epiprogoitrin and progoitrin not only after oral administration but also after i.v. injection. Progoitrin seemed to undergo relatively extensive metabolism and could be eliminated faster than epiprogoitrin. Additionally, epiprogoitrin is less polar than progoitrin, implying that epiprogoitrin has higher membrane permeability, which may explain why a higher AUC is observed for epiprogoitrin than for progoitrin in vivo [18–22].

Furthermore, the epimers may undergo directional chiral inversion relative to each other in vivo, which may also be one of the reasons for distinct pharmacokinetic profiles between epiprogoitrin and progoitrin. Oral bioavailability was measured by the following equation: $F(\%) = (AUC_{i.g.} \times Dose_{i.v.})/(AUC_{i.v.} \times Dose_{i.g.}) \times 100\ \%$. The significant difference in bioavailability is mainly due to the difference of AUC after i.v. administration. Because the $AUC_{i.g.}$ values of epiprogoitrin and progoitrin have not significant difference. We have repeated the pharmacokinetic study of epiprogoitrin and progoitrin after i.v. administration, and the results are similar. Therefore, the differences in bioavailability are associated with the $AUC_{i.v.}$ values. And to date, the possible reason of the differences in $AUC_{i.v.}$ values may be the structure of analytes. However, chiral

Table 4
Pharmacokinetic parameters of epiprogoitrin and progoitrin after intravenous administration (n = 6) at the dose of 2 mg/kg. Data were expressed as mean ± S.D.

Components	C_{max}(μg/L)	$t_{1/2}$(h)	AUC_{0-t}(μg/L*h)	$AUC_{0-\infty}$(μg/L*h)	MRT_{0-t}(h)	$MRT_{0-\infty}$(h)	Vd(L/kg)	CLz(L/kg /h)
progoitrin	1197.44 ± 284.76	1.11 ± 0.154	767.903 ± 84.712	768.124 ± 84.76	0.827 ± 0.036	0.831 ± 0.035	4.185 ± 0.506	2.629 ± 0.279
epiprogoitrin	3276.483 ± 497.368	2.89 ± 0.53	2558.845 ± 311.21	2563.128 ± 306.943	0.851 ± 0.097	0.941 ± 0.197	7.92 ± 4.56	0.79 ± 0.092

inversion has not yet been reported because these analytes have a similar molecular structure and polarity and the same molecular weight and MS fragments. It is thus challenging to separate them through UHPLC, which is generally used in pharmacokinetic studies with short chromatographic cycles.

4. Conclusions

To the best of our knowledge, we herein for the first time to describe a novel LC–ESI–MS/MS method with a short running time (4 min), high sensitivity (2 ng/mL), and economical sample pretreatment for studying a pair of epimers (progoitrin and epiprogoitrin) in rat plasma. The results facilitate a comprehensive understanding of the behaviour of these two glucosinolate epimers *in vivo* and highlight pharmacokinetic differences between them that have not yet been reported. After oral administration, progoitrin and epiprogoitrin were rapidly absorbed from the gastrointestinal tract and exhibited dose-independent pharmacokinetic behaviour. The oral bioavailability of epiprogoitrin and progoitrin was 7.7 %–9.3 % and 20.1 %–34.1 %, respectively. Furthermore, after i.v. administration, the pharmacokinetic parameters between epiprogoitrin and progoitrin showed significant differences, which could be attributed to chiral inversion and membrane permeability. Further studies are warranted to validate our findings in the near future.

CRediT authorship contribution statement

Yan Xu: Investigation, Formal analysis, Writing - original draft, Writing - review & editing, Methodology. **Jinhang Li:** Investigation. **Yanhong Shi:** Supervision, Investigation. **Li Yang:** Project administration, Funding acquisition. **Zhengtao Wang:** Project administration, Funding acquisition. **Han Han:** Validation, Writing - review & editing, Supervision, Conceptualization. **Rui Wang:** Project administration, Funding acquisition, Supervision.

Declaration of Competing Interest

There are no conflicts of interest to declare.

Acknowledgements

This work was financially supported by National Natural Science Foundation of China (project no. 81573571; 81503223); Shanghai Association for Science and Technology (project no. 15DZ0502601; 17DZ2201800); and “Xing lin” Plan of Shanghai University of Traditional Chinese Medicine.

Appendix A. Supplementary data

Supplementary material related to this article can be found, in the online version, at doi:https://doi.org/10.1016/j.jpba.2020.113356.

References

[1] W. Zhou, X.Y. Zhang, Research progress of Chinese herbal medicine *Radix isatidis* (banlangen), Am. J. Chin. Med. 41 (4) (2013) 743–764.
[2] F.Y. Wei, Extraction, Purification and Antioxidant Enhancing Activity of *Radix isatidis*, 2015.
[3] C. Jie, Z. Luo, H. Chen, M. Wang, C. Yan, Z.F. Mao, G.K. Xiao, H. Kurihara, Y.F. Li, R.R. He, Indirubin, a bisindole alkaloid from *Isatis indigotica*, reduces H_1N_1 susceptibility in stressed mice by regulating MAVS signaling, Oncotarget 8 (62) (2017) 105615–105629.
[4] C.W. Lin, F.J. Tsai, C.H. Tsai, C.C. Lai, L. Wan, T.Y. Ho, C.C. Hsieh, P.D. Chao, Anti-SARS coronavirus 3C-like protease effects of *Isatis indigotica* root and plant-derived phenolic compounds, Antiviral Res. 68 (1) (2005) 36–42.
[5] L.W. He, J.Y. Yang, X.B. Hou, Antiviral activity and chemical composition of n-butanol extract of Isatidis Radix, Chin. Tradit. Herb. Drugs 48 (14) (2017) 2843–2849.
[6] K.C. Lee, M.W. Cheuk, W. Chan, A.W. Lee, Z.Z. Zhao, Z.H. Jiang, Z. Cai, Determination of glucosinolates in traditional Chinese herbs by high-performance liquid chromatography and electrospray ionization mass spectrometry, Anal. Bioanal. Chem. 386 (7–8) (2006) 2225–2232.
[7] Y.H. Shi, Z.Y. Xie, R. Wang, S.J. Huang, Y.M. Li, Z.T. Wang, Quantitative and chemical fingerprint analysis for the quality evaluation of *Isatis indigotica* based on ultra-performance liquid chromatography with photodiode array detector combined with chemometric methods, Int. J. Mol. Sci. 13 (7) (2012) 9035–9050.
[8] F. Xie, Studies on the Change Rule of Glucosinolates in Isatidis Radix and Quality Standard of Fu Fang Banlangen Keli, 2015.
[9] Z.Y. Xie, Y.H. Shi, Z.T. Wang, R. Wang, Y.M. Li, Biotransformation of glucosinolates epiprogoitrin and progoitrin to (R)- and (S)-Goitrin in *Radix isatidis*, J. Agric. Food Chem. 59 (23) (2011) 12467–12472.
[10] J.H. Kim, J.H. Lee, S.M. Jeong, B.H. Lee, I.S. Yoon, J.H. Lee, S.H. Choi, D.H. Kim, T.K. Park, S.Y. Nah, Stereospecific effects of ginsenoside Rg3 epimers on swine coronary artery contractions, Biol. Pharm. Bull. 29 (2) (2006) 365–370.
[11] R. Wu, Q. Ru, L. Chen, B.M. Ma, C.Y. Li, Stereospecificity of ginsenoside Rg3 in the promotion of cellular immunity in hepatoma H22-bearing mice, J. Food Sci. 79 (7) (2014) H1430–H1435.
[12] H.H. Kwok, G.L. Guo, J.K. Lau, Y.K. Cheng, J.R. Wang, Z.H. Jiang, M.H. Keung, N.K. Mak, P.Y. Yue, R.N. Wong, Stereoisomers ginsenosides-20(S)-Rg(3) and -20(R)-Rg(3) differentially induce angiogenesis through peroxisome proliferator-activated receptor-gamma, Biochem. Pharmacol. 83 (7) (2012) 893–902.
[13] E.H. Park, Y.J. Kim, N. Yamabe, S.H. Park, H.K. Kim, H.J. Jang, J.H. Kim, G.J. Cheon, J. Ham, K.S. Kang, Stereospecific anticancer effects of ginsenoside Rg3 epimers isolated from heat-processed American ginseng on human gastric cancer cell, J. Ginseng Res. 38 (1) (2014) 22–27.
[14] M.W. Park, J. Ha, S.H. Chung, 20(S)-ginsenoside Rg3 enhances glucose-stimulated insulin secretion and activates AMPK, Biol. Pharm. Bull. 31 (4) (2008) 748–751.
[15] Y.H. Shi, C. Zheng, J.H. Li, L. Yang, Z.T. Wang, R. Wang, Separation and quantification of four main chiral glucosinolates in Radix Isatidis and its granules using high-performance liquid chromatography/diode array detector coupled with circular dichroism detection, Molecules 23 (6) (2018) 1305.
[16] J.H. Li, Y.H. Shi, Y. Xu, L. Yang, Z.T. Wang, H. Han, R. Wang, Metabolic profiles and pharmacokinetics of goitrin in rats through liquid chromatography combined with electrospray ionization-tandem mass spectrometry, Biomed. Chromatogr. 33 (10) (2019) e4606.
[17] U.S. Department of Health and Human Services, Food and Drug Administration, Center for Drug Evaluation and Research, Center for Veterinary Medicine, Guidance for Industry, Bioanalytical Method Validation.
[18] L.W. Qi, C.Z. Wang, C.S. Yuan, American ginseng: potential structure-function relationship in cancer chemoprevention, Biochem. Pharmacol. 80 (7) (2010) 947–954.
[19] S.H. Bae, J.B. Park, Y.F. Zheng, M.J. Jang, S.O. Kim, J.Y. Kim, Y.H. Yoo, K.D. Yoon, E. Oh, S.K. Bae, Pharmacokinetics and tissue distribution of ginsenoside Rh2 and Rg3 epimers after oral administration of BST204, a purified ginseng dry extract, in rats, Xenobiotica 44 (12) (2014) 1099–1107.
[20] J. Liu, J. Shiono, K. Shimizu, H. Yu, C. Zhang, F. Jin, R. Kondo, 20(R)-ginsenoside Rh2, not 20(S), is a selective osteoclastgenesis inhibitor without any cytotoxicity, Bioorg. Med. Chem. Lett. 19 (12) (2009) 3320–3323.
[21] M. Yan, P.F. Fang, H.D. Li, M. Zheng, P. Xu, L.F. Li, Effect of 18α-glycyrrhetinic acid on outward transport of talinoloi in Caco-2 cell monolayers, Chin. Hosp. Pharm. J. 36 (6) (2012) 405–409.
[22] M. Peng, X.N. Li, T. Zhang, Y. Ding, Y.X. Yi, J. Le, Y.J. Yang, X.J. Chen, Stereoselective pharmacokinetic and metabolism studies of 20(S)- and 20(R)-ginsenoside Rg3 epimers in rat plasma by liquid chromatography-electrospray ionization mass spectrometry, J. Pharm. Biomed. Anal. 121 (2016) 215–224.